substance: Ce_2S_3
property: crystal structure, physical properties

α-Ce_2S_3

crystal structure	orthorhombic (D_{2h}^{16} – Pnma)			
lattice parameters				
a	7.55 Å			71B
b	15.79 Å			
c	4.14 Å			

β-Ce_2S_3

crystal structure	tetragonal (D_{4h}^{20} – $I4_1/acd$)		transition α-phase to β-phase at 1410°C	66M
lattice parameters				
a	15.30 Å			71B
c	20.29 Å			
melting point				
T_m	1700°C			60P

γ-Ce_2S_3

crystal structure	cubic (Th_3P_4-defect structure, T_d^6 – $I\bar{4}3d$)			
lattice parameters				
a	8.634 Å			85Z
	8.631 Å			81K
	8.630 Å			65F
	8.6084 Å		from neutron diffraction	71A
melting point				
T_m	2060°C			65F
	1870°C			81K
	2296°C			72G
density				
d	5.31 g cm^{-3}			81K
linear thermal expansion coefficient				
α	$13.2 \cdot 10^{-6}$ K^{-1}			66D
thermal conductivity				
κ	$3.52 \cdot 10^{-2}$ Wcm^{-1} K^{-1}			72C
energy gap and other energy parameters				
E_g	2.06 eV		optical energy gap	64K
	2.0 eV		optical energy gap	67H
	2.7 ± 0.25 eV		thermodynamic	85Z
	1.8 eV		X-ray spectra	83S
E_b	5.3 eV	S 3p-level	MgKα XPS, Fig. 4 (E_b rel. to E_F)	91K
	2.5 eV	Ce 4f-level	MgKα XPS, Fig. 4	
	13.3 eV	S 3s-level	MgKα XPS, Fig. 4	
	19.6 eV	Ce $5p_{3/2}$-level	MgKα XPS, Fig. 4	
	22.6 eV	Ce $5p_{1/2}$-level	MgKα XPS, Fig. 4	
	38 eV	Ce 5s-level	MgKα XPS, Fig. 4	
	108 eV	Ce $4d_{5/2}$-level	MgKα XPS, Fig. 5	

	112 eV	Ce $4d_{3/2}$-level	MgKα XPS, Fig. 5	
E	8.3 eV	S 3p-E_F	ELS, Fig. 6	91K
	11.3 eV	S 3p-cond. band, surface plasmon	ELS, Fig. 6	
	16.4 eV	bulk plasmon	ELS, Fig. 6	
	21.4 eV	Ce 5p-E_F	ELS, Fig. 6	
	30.4 eV	Ce 5p-5d	ELS, Fig. 6	
	≈ 39 eV	Ce 5s-E_F	ELS, Fig. 6	

electrical conductivity

σ	$10^{-10}\ \Omega^{-1}\ cm^{-1}$			71A

activation energy

E_A	2.23 eV		from electrical conductivity	67M

Further igures and references:

coordination polyhedra: Fig. 1

heat capacity: Fig. 2

temperature dependence of **resistivity**: Fig. 3

References:

60P Picon, M., Domange, L., Flahaut, J., Guittard, M., Patrie, M.: Bull. Soc. Chim. Fr. 2 (1960) 221.
64C Cutler, M., Leavy, J. F.: Phys. Rev. 133 (1964) A 1153.
64K Kurnick, S.W., Meyer, C.: J. Phys. Solids 25 (1964) 115.
65F Flahaut, J., Guittard, M., Patrie, M., Pardo, M. P., Golabi, S. M., Domange, L.: Acta. Cryst. 19 (1965) 14.
66D Dudnik, E. M., Lashkarev, G. V., Paderno, Y. B., Obolonchik, V. A.: Inorg. Mater. 2 (1966) 833.
66H Holtzberg, F., Methfessel, S.: J. Appl. Phys. 37 (1966) 1433.
66M Marcon, J. P., Pascard, R.: J. Inorg. Nucl. Chem. 28 (1966) 2551.
67H Henderson ,J.R., Muramoto, M., Loh, E., Gruber, J.B.: J. Chem. Phys. 47 (1967) 3347.
67M Marchenko, V. I., Samsonov, G. V.: Chem. Bond in Semicond. and Solids (ed. N. N. Sirota) New York: Consultants Bureau 1967.
71A Atoji, M.: J. Chem. Phys. 54 (1971) 3226.
71B Besancon, P.: Doctor Thesis, Univ. René Descartes, Paris 1971.
72C Chatterjee, A., Singh, A. K., Jayaraman, A.: Phys. Rev. B 6 (1972) 2285.
72G Goryachev, Yu. M., Kutsenok, T. G.: High Temp. High Press. 4 (1972) 663.
72S Smirnov, I. A.: Phys. Status Solidi (a) 14 (1972) 363.
81K Kamarzin, A. A., Mironov, K. E., Sokolov, V. V., Malovitskii, Y. N., Vasil'yeva, I. G.: J. Cryst. Growth 52 (1981) 619.
83S Soldatov, A.V., Gusatinskii, A.N., Karin, M.G., Sidorin, K.K., Sadovskaya, O.A.: Inorg. Mater. 19 (1983) 951-954.
85Z Zhuze, V.P., Karin, M.G., Sidorin, K.K., Sokolov, V.V., Shelykh, A.I.: Sov. Phys. Solid State 27(12) (1985) 2205.
91K Kaciulis, S., Latisenka, A., Plesanovas A.: Surf. Sci. 251/252 (1991) 330.

Fig. 1.

Th_3P_4-type compounds. The coordination polyhedra of the cations and the anions. Full circles: Th- atoms, other circles: P-atoms [66H].

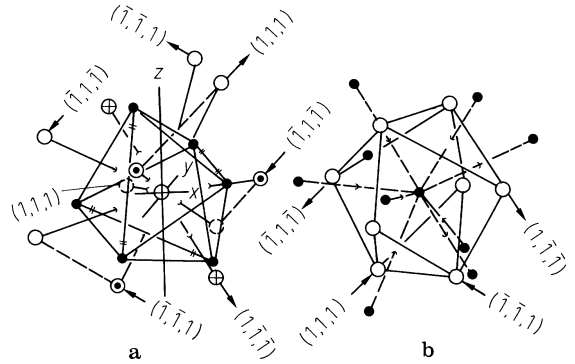

Fig. 2.

γ-Ce_2S_3. Temperature dependence of the molar heat capacity [72S].

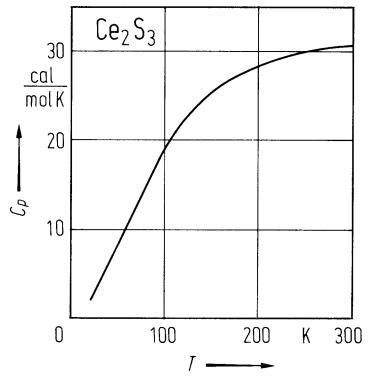

Fig. 3.

γ-Ce_2S_3. Low temperature resistivity vs. reciprocal temperature. For curves a and b the electron concentrations are $8.7 \cdot 10^{17}$ cm^{-3} and $5 \cdot 10^{17}$ cm^{-3}, respectively [64C].

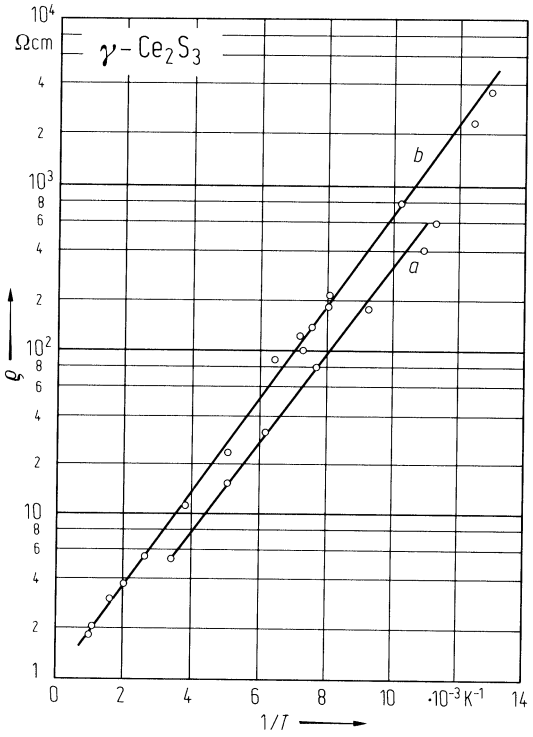

Fig. 4.

γ-Ln_2S_3. MgK_α X-ray photoelectron spectra of the rare-earth sesquisulfides (Ln = La, Ce, Nd, Sm, Gd, Dy) in the energy region below Fermi level down to Ln 5s core level [91K].

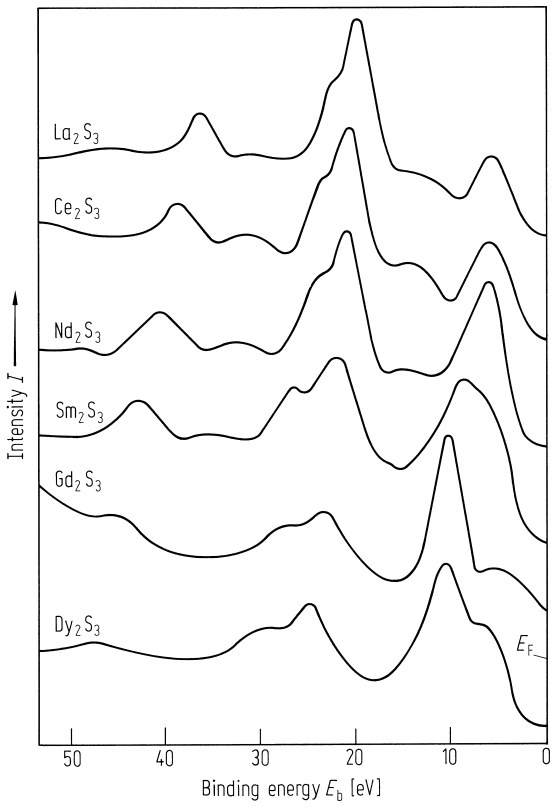

Fig. 5.

γ-Ln_2S_3. MgK_α X-ray photoelectron spectra of the rare-earth sesquisulfides (Ln = La, Ce, Nd, Sm, Gd, Dy) in the 4d core level region [91K]. E_b relative to E_F.

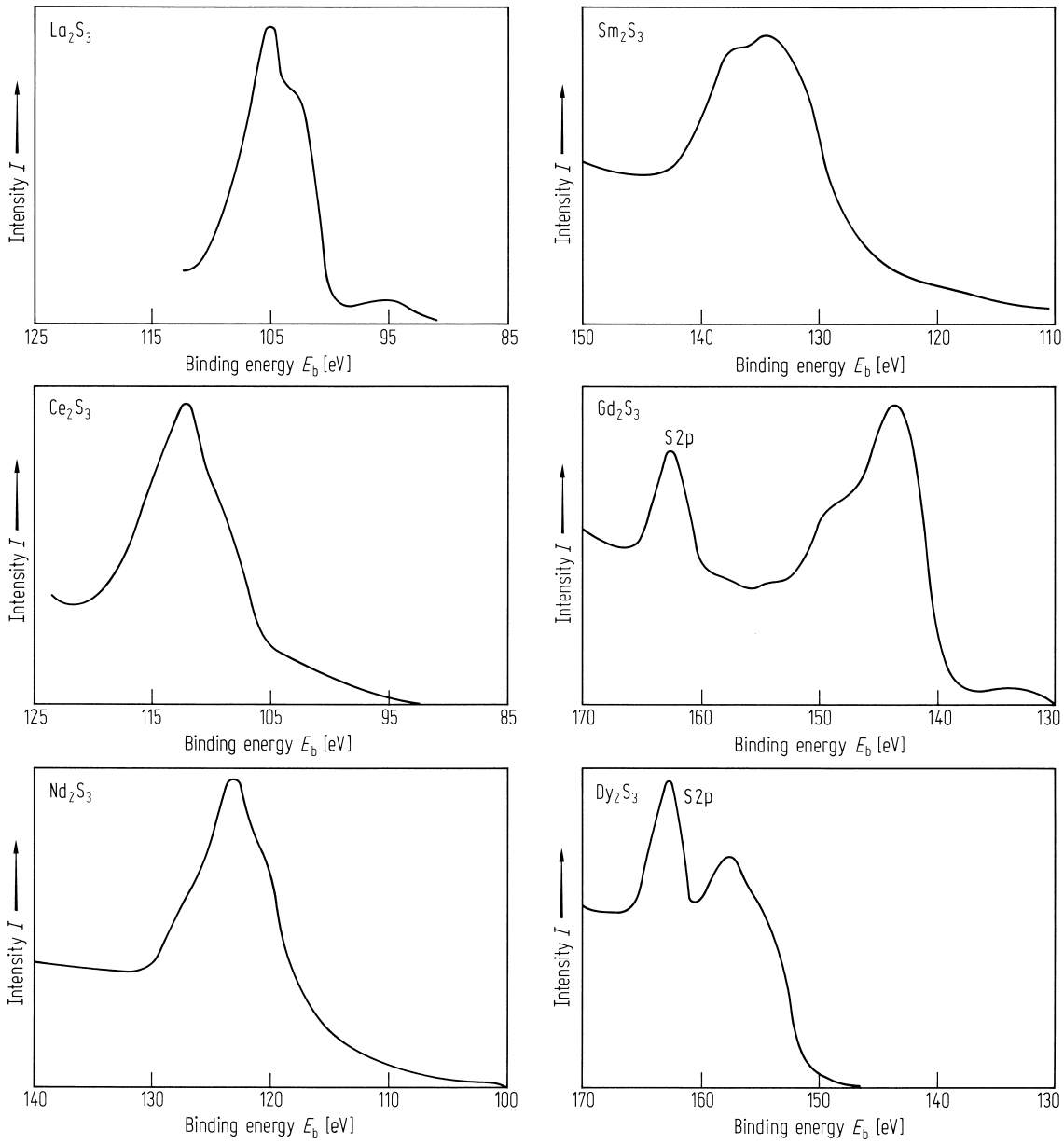

Fig. 6.

γ-Ln_2S_3. Electron loss spectra of the rare-earth sesquisulfides (Ln = La, Ce, Nd, Sm, Gd, Dy) for primary electron beam energy E_p = 750 eV. All the peaks, revealed from the second derivative d^2N/dE^2 are indicated by arrows [91K].